Research Paper

Deposition, deformation, and flexure in a transpressional trough, Queen Charlotte fault, offshore Haida Gwaii (British Columbia, Canada)

Kristin M.M. Rohr[1], Michael Riedel[2], and Kevin P. Furlong[3]

[1]Geological Survey of Canada–Pacific Division, Natural Resources Canada, 9860 West Saanich Road, Sidney, BC V8L 4B2, Canada
[2]GEOMAR Helmholtz Center for Ocean Research Kiel, Wischhofstrasse 1-3, 24148 Kiel, Germany
[3]Department of Geosciences, Pennsylvania State University, 201 Old Main, University Park, Pennsylvania 16801, USA

ABSTRACT

Transpressional deformation along the Pacific–North American plate boundary off British Columbia (Canada) generates interactions between tectonic and depositional processes; first-order deformation is creation of a bathymetric trough by flexure of the Pacific plate. Interpretation of a suite of single-channel seismic reflection data in the central and southern trough shows second-order internal structure and depositional systems within the trough. Much of these sediments originated from Quaternary slope fans, although the age of the underlying oceanic crust is 8–13 Ma. These turbidite deposits overlie hemipelagic deposits. Two distinct layers of turbidite deposits in the trough can be explained by sediment deposition systems rather than tectonic events. We infer that the most recent flat-lying deposits, which have been previously interpreted in the northern trough as indicating a lack of compressive deformation, consist, in fact, of along-axis flows based on the general geomorphology of the margin. Second-order deformation consists of small-offset extensional and compressive structures common within 15 km of the foot of the continental slope. A few normal faults are observed tens of kilometers further out on the flexural bulge. Recent faults that cut the seafloor are observed offshore from the rupture plane of the 2012 M7.8 earthquake and match an area of extensional aftershocks. These faults may not be from bending of the entire bulge, which is 30–40 km wide, but from the plate being pulled into the underthrust zone. Maximum depression of the Pacific plate is also offshore from the region of recent rupture, indicating that this rupture is representative of long-term geologic processes.

■ INTRODUCTION

The sedimentary record of the flexed Pacific plate offshore from Haida Gwaii (British Columbia, Canada) is a prime example of the interactions of voluminous Quaternary sedimentation and tectonic deformation that occur throughout the northern Pacific Ocean. The Pacific–North American plate boundary is strike slip with a component of compression that varies along

Kristin Rohr https://orcid.org/0000-0001-6347-712X

its length (Hyndman, 2015). It is very active seismically (Cassidy et al., 2014) and is located at or near the continental shelf break (Barrie et al., 2013). The architecture of sedimentary systems is commonly taken as an indication of tectonic activity or lack thereof, but sedimentary systems with high deposition rates can create their own structures and mask tectonic features that have small offsets (e.g., Nedimović et al., 2009). The latter has been shown to be true in the Juan de Fuca plate, which is subject to small-offset cooling and flexural faults (Han et al., 2016) as well as recent high-volume deposition from the Astoria and Nitinat fans (Rohr et al., 2019). In the northern Juan de Fuca plate, bending faults are not commonly observed in the deposits of the Nitinat fan (Rohr et al., 2019). When deposition rates are high, sediments can mask faults with offsets smaller than the resolution of the wavelengths used in recording seismic reflection data (Nedimović et al., 2009; Rohr et al., 2019).

The general morphology of the bathymetric Queen Charlotte trough is known, but details have yet to be mapped with multibeam data. Understanding sedimentation patterns is critical to correctly distinguish between sedimentary and tectonic processes and thereby infer geologic evolution. In addition, mechanical properties of sediments in the trough throughout its history will affect the occurrence of earthquakes and landslides (e.g., Moore et al., 2015) and their lateral variability. However, sedimentation in the trough has received little to no study. New data acquisition dedicated to studying sedimentary processes may help to assess wider implications of these processes on geohazards within the region. However, within the current limits of data availability and quality, such linkages remain hypothetical.

Walton et al. (2015) mapped flexure of the Pacific plate from roughly 52°N to 58°N as well as normal faults observed in the lower sedimentary section. While they had good coverage of the northern region, data south of 53.4°N consisted of a single line that ran along strike of the trough. They interpreted undeformed horizons in the trough and a lack of shallow normal faults to be the result of diminished compressive tectonic interactions. Our study looks at many lines across the central and southern trough and maps flexure, folding, and faulting. We also observe flat-lying horizons and few shallow faults, but in this most compressive portion of the plate boundary, we cannot explain them by a lack of compressive deformation. In this paper, we infer that sedimentary processes are primarily responsible.

■ REGIONAL SETTING

The plate boundary between the Pacific and North American plates (Fig. 1) west of Haida Gwaii consists of the long-standing Queen Charlotte fault (Wilson, 1965; Brothers et al., 2019) and the more recently formed Revere-Dellwood fault (Rohr, 2015). On the southwest, the plate boundary is bordered by the Queen Charlotte terrace and trough of the Pacific plate (Chase and Tiffin, 1972), and to the northeast, by the islands of Haida Gwaii (Woodsworth, 1991) and the Queen Charlotte Basin of North America (Rohr and Dietrich, 1992).

The relative plate motions between the Pacific and North American plates west of Haida Gwaii (Fig. 1) are transpressive; the curved shape of the Queen Charlotte fault results in a greater degree of compression in its southern end that becomes nearly pure strike slip west of the Alaska panhandle. Computations of relative plate motions have taken different approaches: whole plate
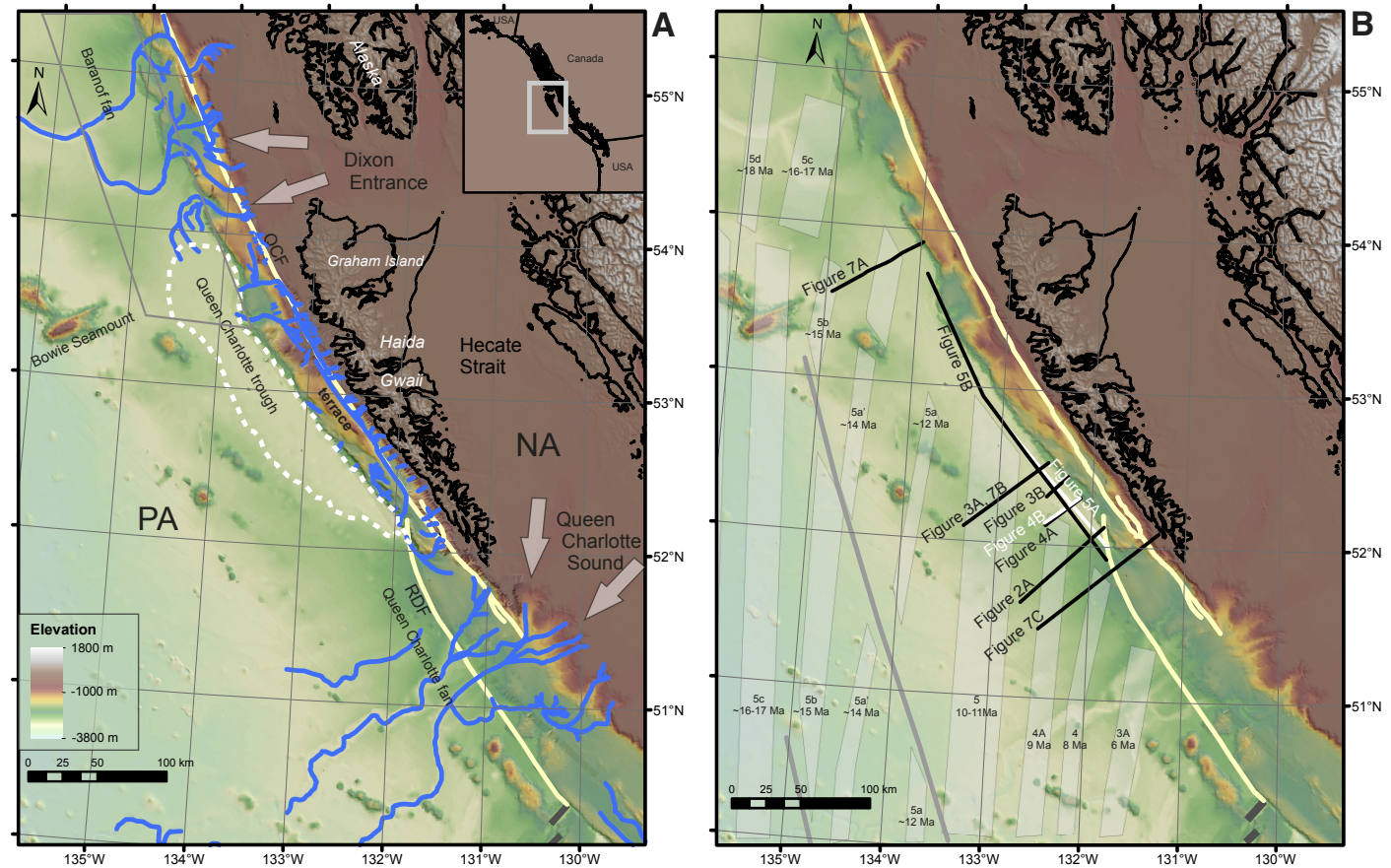

Figure 1. (A) Haida Gwaii (British Columbia, Canada) diverts North American (NA) sediments from reaching flexural Queen Charlotte trough (white dashed line on 2800 m contour) or abyssal plain west of the islands. Numerous gullies (blue lines) south and north of Haida Gwaii feed Queen Charlotte and Baranof slope fans; broad white arrows show direction of flow. On continental slope, not every gully was drawn because there were too many between Pacific (PA) plate and North American plate (Harris et al., 2014). Plate boundary consists of Queen Charlotte fault (QCF) and Revere-Dellwood fault (RDF) (yellow lines). Thin gray line denotes area of depth-to-basement map in Walton et al. (2015). Bathymetry is combination of Global Multi-Resolution Topography (Ryan et al., 2009) downloaded from GeoMapApp (https://www.geomapapp.org) and Geological Survey of Canada multibeam data of Queen Charlotte fault (Barrie et al., 2013). (B) Magnetic anomaly interpretations (light gray polygons) after Wilson (2002). Rift propagators are denoted as gray lines.

circuit (DeMets and Merkouriev, 2016) and morphologic (Brothers et al., 2019). The most recent plate circuit model (DeMets and Merkouriev, 2016) computed that at a latitude of 53°N where the azimuth of the Queen Charlotte fault is 320° clockwise from north, compression began ~11–12 Ma, increased ~6 Ma, and held steady after 3 Ma. The current net rate is 48.3 mm/yr; the compressive component is 14.7 mm/yr. A geomorphic study of the Queen Charlotte fault in the Holocene (Brothers et al., 2019) computed a rate of 51.6 mm/yr for this same location and a compressive component of 6.8 mm/yr. In general, the morphologic model has resulted in faster and less compressive relative plate motions between the North American and Pacific plates, but it is not clear how far back in time these numbers are applicable.

Seismicity occurs along the Queen Charlotte fault as well as in the terrace and adjacent islands. Focal mechanisms determined by composite solutions (Bérubé et al., 1989; Bird, 1997) and moment tensor analysis (Ristau et al., 2007) reveal strike-slip, compressional, and extensional mechanisms, as expected in a region of distributed strike-slip deformation. A M7.8 oblique thrust earthquake occurred in 2012 (Cassidy et al., 2014) and was followed by numerous aftershocks including many normal fault mechanisms in the trough (Kao et al., 2015).

Transpression created both a trough available for deposition of sediments in glacial runoff as well as a barrier to that deposition in the form of an uplifted edge of North America, i.e., Haida Gwaii (Hyndman, 2015; Schoettle-Greene et al., 2020). Sediments have flowed around the archipelago (Barrie et al., 2021), eroding canyons, gullies, and channels into the adjacent continental shelf and abyssal plain (Fig. 1). Transpression has also folded and faulted sediments into the Queen Charlotte terrace, which is often likened to an accretionary prism (Hyndman, 2015).

Flexure of the Pacific plate has been studied off northern Haida Gwaii to assess plate interactions with North America (Prims et al., 1997) and the effects of the Kodiak-Bowie (Pratt-Welker) seamount chain (Harris and Chapman, 1994). The former study was based on a multichannel seismic reflection profile that crossed the trough at 54°N and interpreted that the plate had an elastic thickness of ~15 km. The latter study had only a few locations with interpreted sediment thickness and interpreted an elastic thickness of ~12 ± 5 km off northern Haida Gwaii. These are as expected for 10–15 Ma oceanic lithosphere (Harris and Chapman, 1994). Harris and Chapman (1994) concluded that many of the seamounts formed near the ridge and do not appear to have altered the flexural strength of the plate off northern Haida Gwaii. The southern trough was not included in either study because of a lack of knowledge of sediment thickness and superposition of seamount and trough flexural signatures.

The Queen Charlotte trough has formed from the interplay of cooling, elastic flexure of the Pacific plate, and sedimentation processes (Han et al., 2016; Hyndman, 2015). Sedimentation has not filled the trough, so it can be defined by the 2800 m contour in bathymetry (Fig. 1); it is as much as 2950 m deep along axis. At the southern end, it is bound by the Revere-Dellwood fault and the Queen Charlotte slope fan which originates from Queen Charlotte Sound; here the trough is a small notch that over a short distance widens to 30 km

(Davis and Seemann, 1981). On most of its 250 km length, it is 35–40 km wide. At the northern end, it is bound by the Baranof fan, which originates locally from Dixon Entrance; the fan filled in the trough and further depressed the flexed plate (Walton et al., 2015).

Slope fans north and south of Haida Gwaii (Fig. 1) consist mainly of glacial melt runoff (Barrie et al., 2021; Walton et al., 2014; Chase and Tiffin, 1972). They are being translated north along the plate boundary (Brothers et al., 2019), which elongates the classic fan shape. Deposits offshore from Dixon Entrance are as thick as 4 s two-way travel time (~5 km) thick (Walton et al., 2015). A lack of shallow faulting was interpreted by Walton et al. (2015) as an indication of a lack of recent compressive deformation. Regional bathymetry and multibeam data (Srivastava et al., 1971; GeoMapApp, https://www.geomapapp.org; Ferguson et al., 2018; Zhang and Gulick, 2019) have imaged channel levee complexes from both fans that extend hundreds of kilometers onto the Pacific plate. Distal deposits as well as fallout from suspended sedimentary plumes reach the Pacific plate west of Haida Gwaii; these deposits would be expected to be fine grained.

Glacial history is variable within the region (Barrie et al., 2021; Barrie and Conway, 1999). Ice masses are thought to have reached the shelf edge in the Last Glacial Maximum north and south of Haida Gwaii, effectively removing most of the evidence of previous glaciations. Small ice masses on Haida Gwaii were probably not large contributors of sediment volume during deglaciation (15–10 ka) (Barrie et al., 2021). Any contributions from the west side of Haida Gwaii would have flowed along a valley created by the Queen Charlotte fault and into the trough (Barrie et al., 2021). The runoff divide of Haida Gwaii is close to the west coast, such that most of the sediments eroded from Haida Gwaii were washed into Hecate Strait and then into the Queen Charlotte fan.

■ DATA

We focus on data collected west of southern Haida Gwaii in order to study flexure and structure where the Pacific plate experiences the greatest compression relative to North America. Reflection data acquisition in the region spans 1969–2013; the data were recorded mostly on a single channel, although one line used two channels (Bruns et al., 1992). Many of the lines interpreted here have been previously published (Srivastava et al., 1971; Chase and Tiffin, 1972; Davis and Seemann, 1981; Carbotte et al., 1989; Riedel et al., 2019, 2020) but largely without any interpretations on the sections (i.e., major features were described in the text). When describing the lines, we will use the distance (offset) along the line, the *x*-axis, as a reference for various features.

Legacy data collected by University of British Columbia and the Geological Survey of Canada in 1969 (Srivastava et al., 1971), 1971 (Chase and Tiffin, 1972), 1972 (Carbotte et al., 1989), 1973, and 1978 (Davis and Seemann, 1981) were scanned from paper records and vectorized into SEGY (Society of Exploration Geophysicists) format files. The resulting data can be interpreted digitally in

a program but not filtered or processed. Lines 86-1 and 86-3 were scanned from photographic negatives of the paper sections and then vectorized; these reflection lines have never been published before. In scanned lines, it can be difficult to detect subtleties such as onlap of reflectors in the fanned and faulted sedimentary sections. Navigation before 1994 was by Loran (long-range navigation) with occasional satellite fixes; later, GPS was used, and by 2001, real-time GPS was used. Depth of the seafloor in the seismic reflection data was checked against modern bathymetry maps to ensure that the data were located correctly.

Seismic reflection data from 1994 and 2013 were acquired digitally in the field at 4 and 1 ms sample rates using a 655 cm³ and a 8521 cm³ airgun, respectively (Riedel et al., 2014). Two-channel data were collected by the U.S. Geological Survey on strike lines during acquisition of GLORIA sonar data (Bruns et al., 1992); the source was a 2622 cm³ airgun and had a signature ~200 ms long.

The frequency content varied from 30 to 140 Hz in the various data sets and was typically 70 Hz for the 1978 data set, which comprised the most lines in the region. This results in vertical resolution of 3–4 m for data in the upper half second, assuming velocities of 1600–2100 m/s.

■ OBSERVATIONS AND INTERPRETATIONS

The resulting collection of legacy data has an average line spacing of ~18 km. Most of the lines are perpendicular to the strike of the coast, although several strike lines allow horizon interpretations to be tied.

Abyssal Plain

Observations of sediment waves on the abyssal plain (Fig. 2) allow us to infer that a large volume of the sediments in the trough was deposited in a Quaternary slope fan (Wynn and Stow, 2002; Normark et al., 2002). Surficial deep-water facies of the Queen Charlotte fan include sediment waves, e.g., along profile 15 in Davis and Seemann (1981); these indicate that fast high-density fluids flowed down the fan and onto the abyssal plain. West of Haida Gwaii (Fig. 2C), they can be seen on the seafloor in multibeam data 70–90 km from the shelf edge (Norgard et al., 2019). Seismic reflection data show (Fig. 2B) that they can be observed as far down as 330 ms below seafloor (bsf) and deeper (e.g., 45 km, 400 ms bsf; and possibly 75 km, 650 ms bsf; Fig. 2A). These latter observations indicate that sediment dynamics similar to those close to the shelf edge were active when these deeper sediments were deposited. Because glacial melt episodes generate fast flow (Pickering and Hiscott, 2016), we infer that the deeper sediment waves were also deposited from fast-moving glacial melt and are, therefore, Quaternary. These sediments represent a portion of time in the Quaternary—but not necessarily the entire period. Not all Quaternary sediments occur as sediment waves. Turbidite deposits from the fan would show up in the seismic record as laterally extensive layers with

small- to large-amplitude reflectors. These can be seen closer to the shelf edge in this profile, e.g., from 65 to 80 km in Figure 2A. The fan thickens toward North America to as much as 700 ms.

The base of sediment waves can be tracked through this profile; laterally, reflectors are from smoother turbidite deposits (Fig. 2A) that thicken toward land. This thickening is most likely from a sedimentary process because basement is nearly flat lying; in some interpretations, such thickening has been taken as evidence of tectonic flexure (e.g., Walton et al., 2015). The turbidites lie above a more homogeneous layer of overall small reflection amplitudes of what are most likely hemipelagic sediments, typical of the broad abyssal plain. Basement is sporadically imaged 500–700 ms below the fan. Near the trough, approximately half of the sediments are Quaternary (<2.6 Ma) in age even though oceanic basement is 7.5–11 Ma (Atwater and Severinghaus, 1989; Wilson, 2002), testament to high deposition rates during the Quaternary.

Dip Lines across the Trough

Reflection profiles across the trough show significant landward deflection of the oceanic plate and mild deformation in the sediments. These features have been described in individual lines before, but looking at the entire suite of data in a digital interpretation package allows us to map a general three-dimensional pattern of depositional history, plate flexure, and deformation. We convert time to depth for a sedimentary fill sequence as well as depth to basement to show along-strike variations in plate flexure.

Line 86-1

In line 86-1 (Fig. 3A), the oceanic plate is substantially deflected downward over a distance of only 30 km. To the west, sediments thicken toward a small seamount, giving a false impression of where flexure begins. The seamount is part of the Kodiak-Bowie chain (Chaytor et al., 2007; Norgard et al., 2019). Basement is minimally deflected between the seamount and 32 km distance along the profile shown. Two main sedimentary units are visible: A deeper deformed unit that has been flexed down into the trough, and a unit that is filling the trough. Above basement, an ~0.8-s-thick parallel-bedded sedimentary section between 32 and 45 km distance has been bent conformable with basement into the trough. One normal growth fault (at 45 km) cuts the seafloor, sediments, and basement. Between it and the base of the slope just 12 km away, the lower sediments are difficult to see clearly but are nearly parallel to basement. Above them, sediments fan toward the slope and are faulted and folded. Closer to the terrace, some faults have a reverse sense of motion and have created slight folds in the sediments (at 45 and 48 km between 4.5 and 5.3 s). Folds diminish in amplitude upwards in shallower sediments. Incipient thrusts are not unusual in the compressive setting of subduction trenches
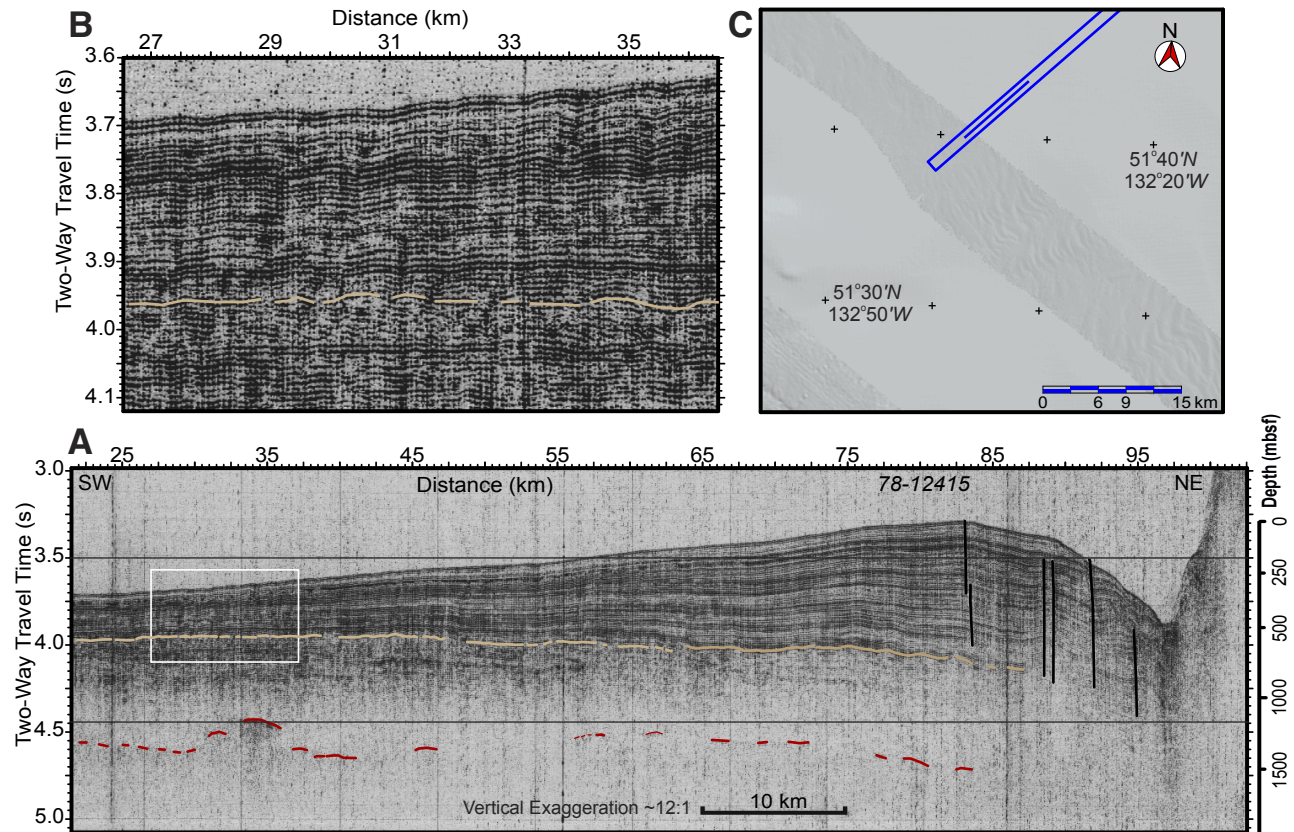
Figure 2. Sediment waves (interpreted following Pickering and Hiscott, 2016; Wynn and Stow, 2002) exist on Pacific plate as far as 70–90 km from shelf edge. (A) Seismic reflection line 78-12415 across Queen Charlotte fan that has been laterally transported to northwest. Uppermost section consists of layered turbidites; lowermost less-reflective section is dominantly hemipelagic deposits. Beginning of flexural trough is evident in northeastern end of the line. Beige line is base of observed sediment waves; red line is top of oceanic basement. Scale on right side is approximate meters below seafloor (mbsf). Location of line is in Figure 1. (B) Detail of line (white box in A) showing surficial and deeper sediment waves. (C) Swath of multibeam data (Norgard, et al., 2019); open blue rectangle is location of line 78-12415; short segment within it is location of detail in B.

(e.g., Cascadia, offshore western North America; Hyndman et al., 1994), but these compressive faults are buried below undeformed sediments, implying that they are no longer active. In Cascadia, incipient thrusts are interpreted to be active, not dormant. Folds in the trough imaged by line 86-1 appear to be confined to older layers (Fig. 3). Sedimentary layers in the top ~200 ms of the trough have fewer faults, are essentially flat lying, and onlap the deflected sediments to the west. These horizons were tracked to many other reflection lines. Basement under the trough is rougher than basement to the west, which is likely the result of faulting.

Sediments on the shoulder (flexural bulge, at ~20–40 km in Fig. 3A) are likely a combination of distal sediments from both the Baranof fan to the north (Zhang and Gulick, 2019) and the Queen Charlotte fan to the south (Ferguson et al., 2018). The Pacific plate has traveled ~125 km northwestward using a relative plate motion rate of 48 mm/yr (DeMets and Merkouriev, 2016) in the Quaternary, when high volumes of sediment were released by melting glaciers. Channel-levee complexes from both fans flow to the southwest (Zhang and Gulick, 2019; Ferguson et al., 2018), but plumes of suspended sediments associated with channel flow can spread widely (Pickering and Hiscott, 2016).
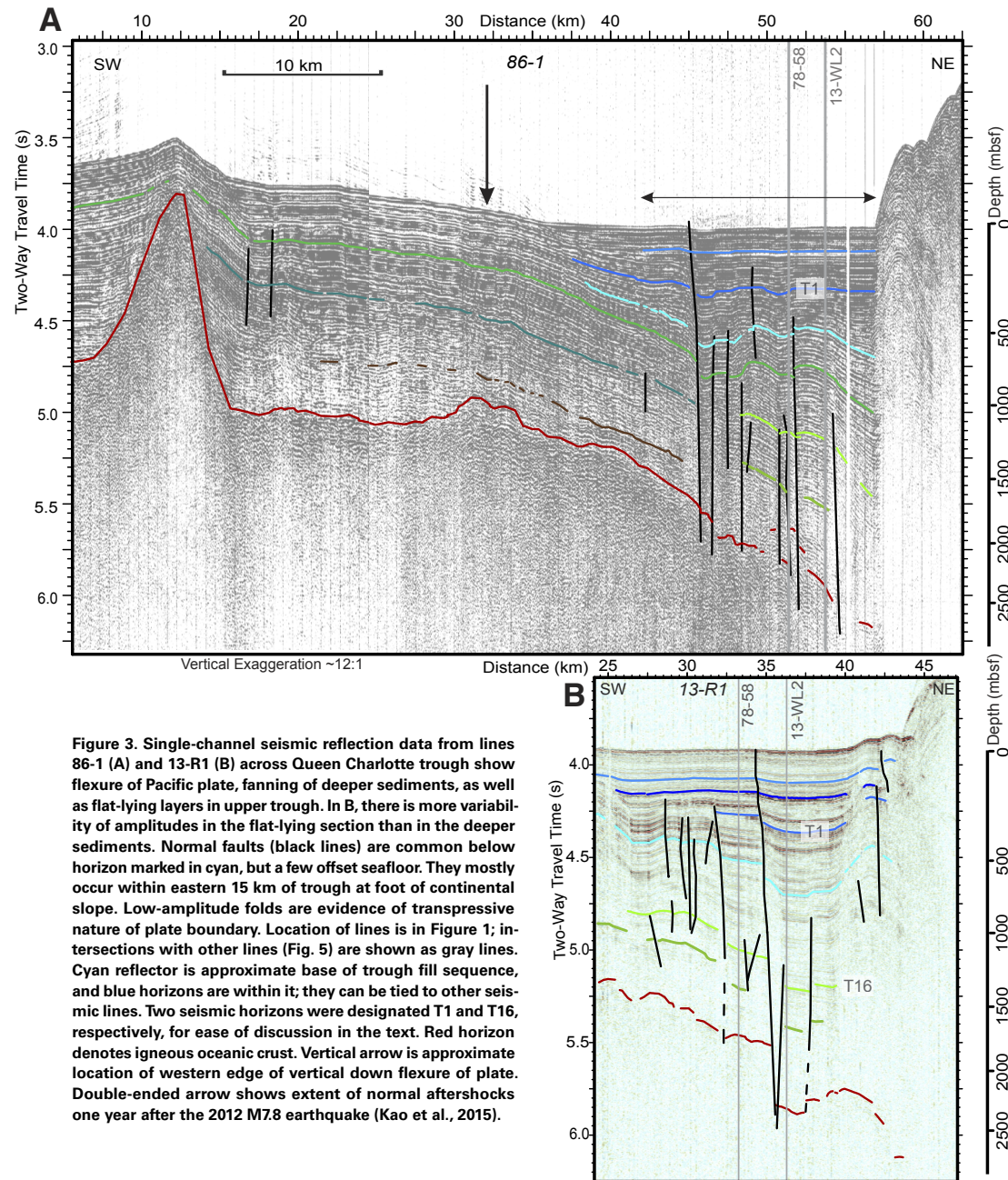
Figure 3. Single-channel seismic reflection data from lines 86-1 (A) and 13-R1 (B) across Queen Charlotte trough show flexure of Pacific plate, fanning of deeper sediments, as well as flat-lying layers in upper trough. In B, there is more variability of amplitudes in the flat-lying section than in the deeper sediments. Normal faults (black lines) are common below horizon marked in cyan, but a few offset seafloor. They mostly occur within eastern 15 km of trough at foot of continental slope. Low-amplitude folds are evidence of transpressive nature of plate boundary. Location of lines is in Figure 1; intersections with other lines (Fig. 5) are shown as gray lines. Cyan reflector is approximate base of trough fill sequence, and blue horizons are within it; they can be tied to other seismic lines. Two seismic horizons were designated T1 and T16, respectively, for ease of discussion in the text. Red horizon denotes igneous oceanic crust. Vertical arrow is approximate location of western edge of vertical down flexure of plate. Double-ended arrow shows extent of normal aftershocks one year after the 2012 M7.8 earthquake (Kao et al., 2015).

Rohr et al. | Deposition in a transpressional trough

6

The Pacific plate has traveled northward from the depositional regime of the Queen Charlotte fan and into the regime of the Baranof fan, so younger sediments are more likely to be from the Baranof fan and older sediments from the Queen Charlotte fan.

Line 13-R1

Line 13-R1 (Riedel et al., 2019) (Fig. 3B) lies just 17 km south of line 86-1. The digital data show the sedimentary and active tectonic structures in more detail than the analogue data such as line 86-1: The mid-depth sediments thicken landward, are cut by several steep faults, and are overlain by nearly flat layers. In addition, the flat unit is more reflective than the deformed unit. The igneous crust is flexed down in the trough, and a steeply dipping extensional growth fault (at 34 km distance along the profile) extends from the seafloor to basement just 11 km from the base of the slope. Significant differences on either side of the fault are visible below horizon T1 (in medium blue in Fig. 3B), which has been offset by 30 ms, and horizon T16 (upper green), which has been offset by ~140 ms. Offset of ~300 ms in basement shows that this is a growth fault (i.e., active during deposition of the sediments). Small reflection amplitudes in the deepest sediments could have been created by spreading loss and absorption of energy from the seismic source and/or by the weakly reflective nature of the presumably hemipelagic sediments (Chase and Tiffin, 1972). An anticline between 39 and 43 km is growing, pushing up the seafloor by ~60 m just seaward of the deformation front. These second-order structures are different from 86-1 as is the presence of faults and folds west of the growth fault.

Lines 71-45 and 78-12290

Of two nearly coincident lines recorded from different sources, one (line 71-45) shows the broad shape of basement dipping underneath the trough (Fig. 4B) (Chase and Tiffin, 1972) and the other (line 78-12290) shows trough fill in some detail (Fig. 4A) (Hyndman and Ellis, 1981). Basement dips landward into the trough by 500 ms between 0 and 15 km on line 71-45. Between 13 and 18 km, out-of-plane reflections from a three-dimensional basement surface have likely been recorded. Even so, there appears to be an offset of ~200 ms of basement by the growth fault that breaks the seafloor (at 19 km in Fig. 4B). Sediments on the western shoulder have low reflectivity and are layered and subparallel, thickening slightly toward land (Fig. 4A). This subtle thickening is likely from deposition in the Queen Charlotte slope fan. More reflective fill in the trough truncates abruptly against the shoulder, suggesting a possible 500 ms fault offset of the shoulder sediments at 80 km (Fig. 4A). In this transition, diffractions and low signal-to-noise values at depth obscure reflectors' geometry. This lateral transition may not be completely created by a fault offset but may be created by sediments in the shoulder interfingering with trough fill and distal fan deposition. Deposition might have occurred simultaneously from different directions. Sediments in the shoulder are subparallel to basement; the fact that they flatten around 65 km (Fig. 4A) suggests that basement has also flattened and that the flexural width here is similar to that seen in line 86-1 (~30 km, Fig. 3A).

A pair of faults in the shoulder can be seen in both lines (68 and 71 km in Fig. 4A, and 4 and 7 km in Fig. 4B). Connecting them across a 2.4 km gap results in a strike direction subparallel to that of the magnetic lineations (Fig. 1B; Riedel et al., 2019, their figure 7). This implies that the original extensional fabric of the oceanic crust is being reactivated during flexure, as is occurring further north (Tréhu et al., 2015).

Strike Lines along the Trough

Line 13-WL2

A strike line composited from several lines collected in 2013 (line 13-WL2; Fig. 5A) (Riedel et al., 2014) begins in the southeast at the Revere-Dellwood fault (130–135 km distance along the profile) and extends 90 km northwest along the trough axis (Fig. 1). Recent northward propagation of the Revere-Dellwood fault (Rohr, 2015) is evident as a number of small-offset faults that disrupt an otherwise coherent set of layers. Between 130 and 85 km, basement is flexed down by ~1 s (~1 km), and further to the northwest, basement shallows slightly by ~0.250 s. Folds and faults deform the horizon indicated in cyan in Figure 5A, deeper sediments, and basement in the trough. Horizons in the deeper unit dip down slightly to the southeast as expected for deposition on a plate being translated past a sediment source (e.g., Nilsen and McLaughlin, 1985). Above the down-flexed cyan horizon, sediments in the more reflective fill unit are essentially flat; they simply fill the depression formed by flexure. They are thickest between 45 and 85 km. Two thin debris flows (as much as 20 ms thick) can be observed on the seafloor 5.5–7 km from the base of the slope; they result from landslides imaged with multibeam data (Greene et al., 2018). In this line, not much detail can be observed in the folded sediments, but layering seems concordant within the fold, implying that deformation happened after much of the deposition. The exception (at 101 km) is a faulted anticline that shows thinning of sediments toward a fault at 103 km. This fault is the only one to offset the fill sequence and the seafloor. The cyan horizon is not a perfect unconformity—there is some thickening between it and the horizon indicated in green below, and it has been folded in its southern expression. It is a horizon that was consistently traced laterally among the different lines.

The deepest sediments appear to have been deposited in the Queen Charlotte fan when the plate was beyond the flexure of the trough (Fig. 2) and translated northwest into the flexed region. Their flexure is clearly observed between 90 and 130 km of Figure 5A. The fill sequence onlaps this monocline (Fig. 5A) so must have been deposited after formation of topography underlying the trough.
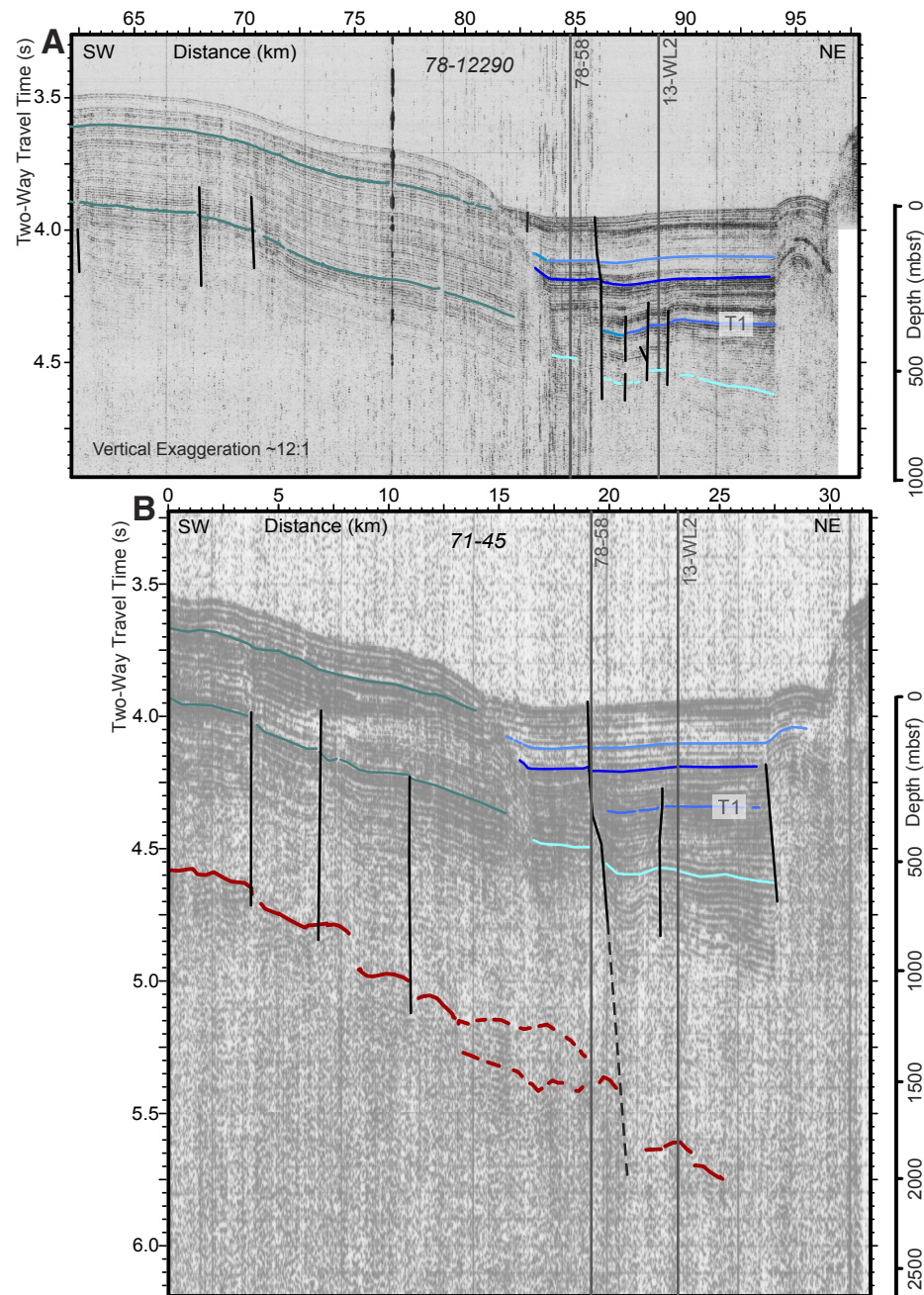
Figure 4. Single-channel seismic reflection data from lines 78-12290 (A) and 71-45 (B) across southern Queen Charlotte trough show difference in reflection character between trough fill sequence and distal turbidites of the flexed plate. Trough fill in A above horizon marked in cyan has higher values of reflections' amplitude as well as greater variability within the section. Reflections are largely clipped because of gain applied in the field to analogue data. In B, a growth fault appears to cut basement (red horizon); dashed and doubled region of basement is probably a result of out-of-plane reflections from rough topography. Location of lines is in Figure 1; intersections with other lines (Fig. 5) are shown as gray lines. A seismic horizon was designated, T1, for ease of discussion in the text. mbsf—meters below sea floor.
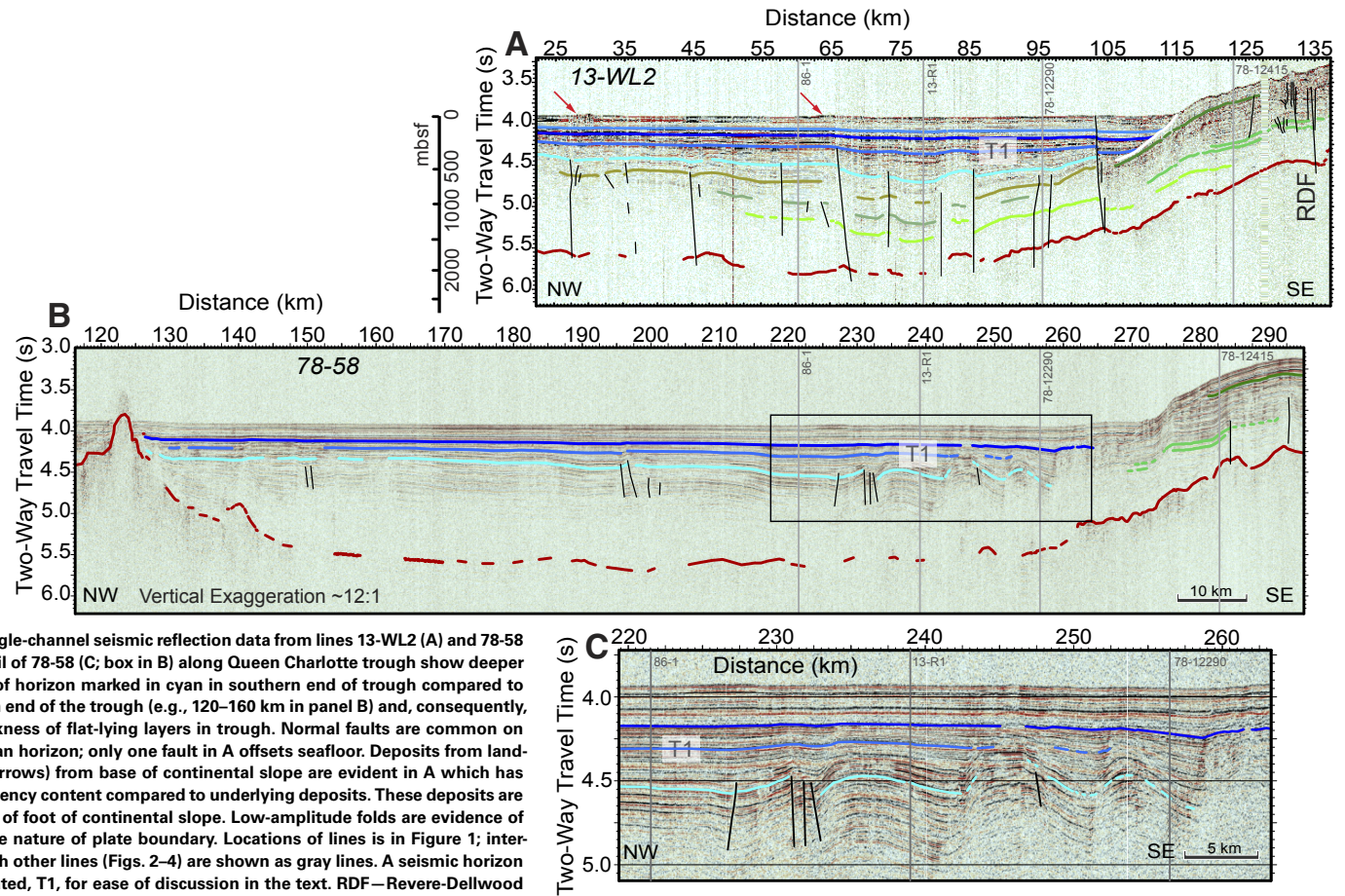
Figure 5. Single-channel seismic reflection data from lines 13-WL2 (A) and 78-58 (B) and detail of 78-58 (C; box in B) along Queen Charlotte trough show deeper occurrence of horizon marked in cyan in southern end of trough compared to the northern end of the trough (e.g., 120–160 km in panel B) and, consequently, greater thickness of flat-lying layers in trough. Normal faults are common on or below cyan horizon; only one fault in A offsets seafloor. Deposits from landslides (red arrows) from base of continental slope are evident in A which has higher-frequency content compared to underlying deposits. These deposits are within 7 km of foot of continental slope. Low-amplitude folds are evidence of transpressive nature of plate boundary. Locations of lines is in Figure 1; intersections with other lines (Figs. 2–4) are shown as gray lines. A seismic horizon was designated, T1, for ease of discussion in the text. RDF—Revere-Dellwood fault; mbsf—meters below sea floor.

Line 78-58

Another strike line, 78-58, shows most remarkably that basement does not change depth much along the trough (Bruns et al., 1992; Walton et al., 2015) (Fig. 5B). The signal-to-noise ratio is admittedly low deep in the section, but cross lines studied here lend confidence to this previous interpretation. The fill sequence onlaps the horizon of the deformed deeper layers (indicated in cyan in Fig. 5B) and is visibly thicker in the southeast. Although strike lines 13-WL2 and 78-58 are 0–5.5 km apart, the folds observed cannot be correlated between the lines. In fact, the anticline at ~245 km in line 78-58 appears to have the opposite vergence of an anticline at 83 km in line 13-WL2. While the veracity of the positions obtained from the navigational system used by the

ship can be questioned, it is likely that these structures are small in scale. The northern end of line 78-58 continued onto the terrace, so a direct tie to lines in the north is not possible.

Flexure, Sedimentation, and Structures in the Trough

Seismic reflection data in the trough allow broad-scale mapping of basement flexure, thickness of the trough fill sequence, and some structures in the trough. From these features, we can infer how the Pacific plate is being deformed as it encounters North America along the Queen Charlotte fault and how that has affected sedimentation patterns.

Flexure

A contoured grid of depth to basement shows that the Pacific plate is flexed downward toward the terrace and that flexure varies along strike (Fig. 6). Travel times of reflections from basement were converted to depth using a velocity profile compiled from clastic sections around the world (Han et al., 2017). In the southernmost area, interactions between the Revere-Dellwood fault and the Queen Charlotte fault have uplifted oceanic basement and generated small-offset faulting; extension in the overlap of the two strike-slip faults has also generated volcanism (Fig. 7C) (Rohr, 2015; Rohr and Furlong, 1995; Allan et al., 1993). From south to north along the axis of the trough, the depth of the oceanic plate seaward of the terrace descends to ~5.5 km below the seafloor

(~52°N), maintains this approximate depth northward, is elevated by sea-mounts (~53°N), and then is depressed under the Baranof fan. Interpretation of several multichannel lines in the north showed basement as deep as 7.5 s (Walton et al., 2015) or >8 km (Prims et al., 1997). Across the trough, basement is deflected by ~2 km between 52°20′N and 53°N on a dip of ~4.4°. There are no lines available that image basement at the base of the slope between maximum flexure (52°30′N) and the seamounts, so the depth-to-basement map may be somewhat skewed by a lack of data.

A comparison of seismic sections (Fig. 7) shows variations in flexure in cross section due to variations in plate age (cooling), sediment load, and degree of compression. Flexure in the two northern lines (Figs. 7A and 7B) is also affected by flexure along the seamount chain (Harris and Chapman, 1994).
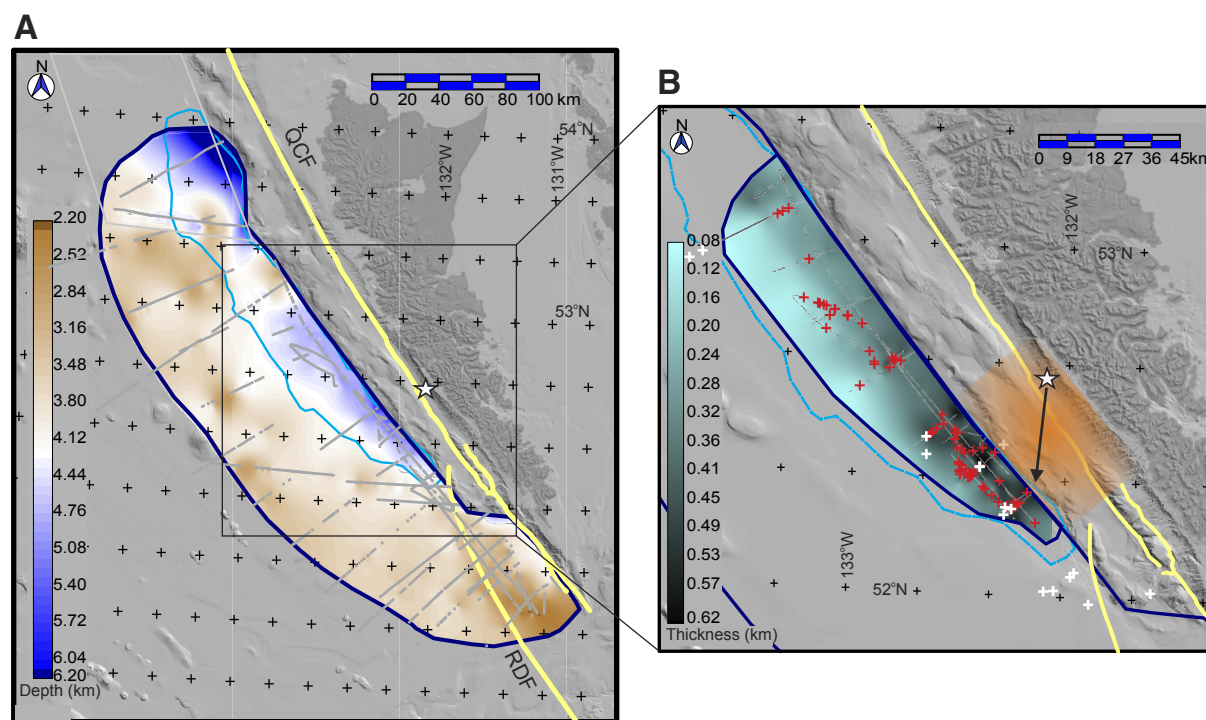

Figure 6. Contour maps of depth to basement (A) and thickness of flat-lying trough fill sequence (B). The former used a generic clastic sediment compaction velocity function (Han et al., 2017), and the latter used a velocity function specific to the trough that describes under-consolidated layers of the trough fill sequence (Riedel et al., 2020). Turquoise dashed line is 2800 m bathymetric contour defining extent of trough. In A, light gray rectangle in northwest denotes area of depth-to-basement map by Walton et al. (2015) in which more than one seismic reflection line was used. White star is location of the 2012 M7.8 earthquake (Kao et al., 2015); black arrow pointing south-southwest is computed rupture direction (Kao et al., 2015). Orange highlights approximate area of rupture surface (Nykolaishen et al., 2015). Gray lines indicate locations of data used in contouring. Red crosses indicate locations of faults that offset horizon marked in cyan in Figures 3–5, and white crosses, the seafloor. Black crosses are placed every 20′ latitude. QCF—Queen Charlotte fault; RDF—Revere-Dellwood fault.
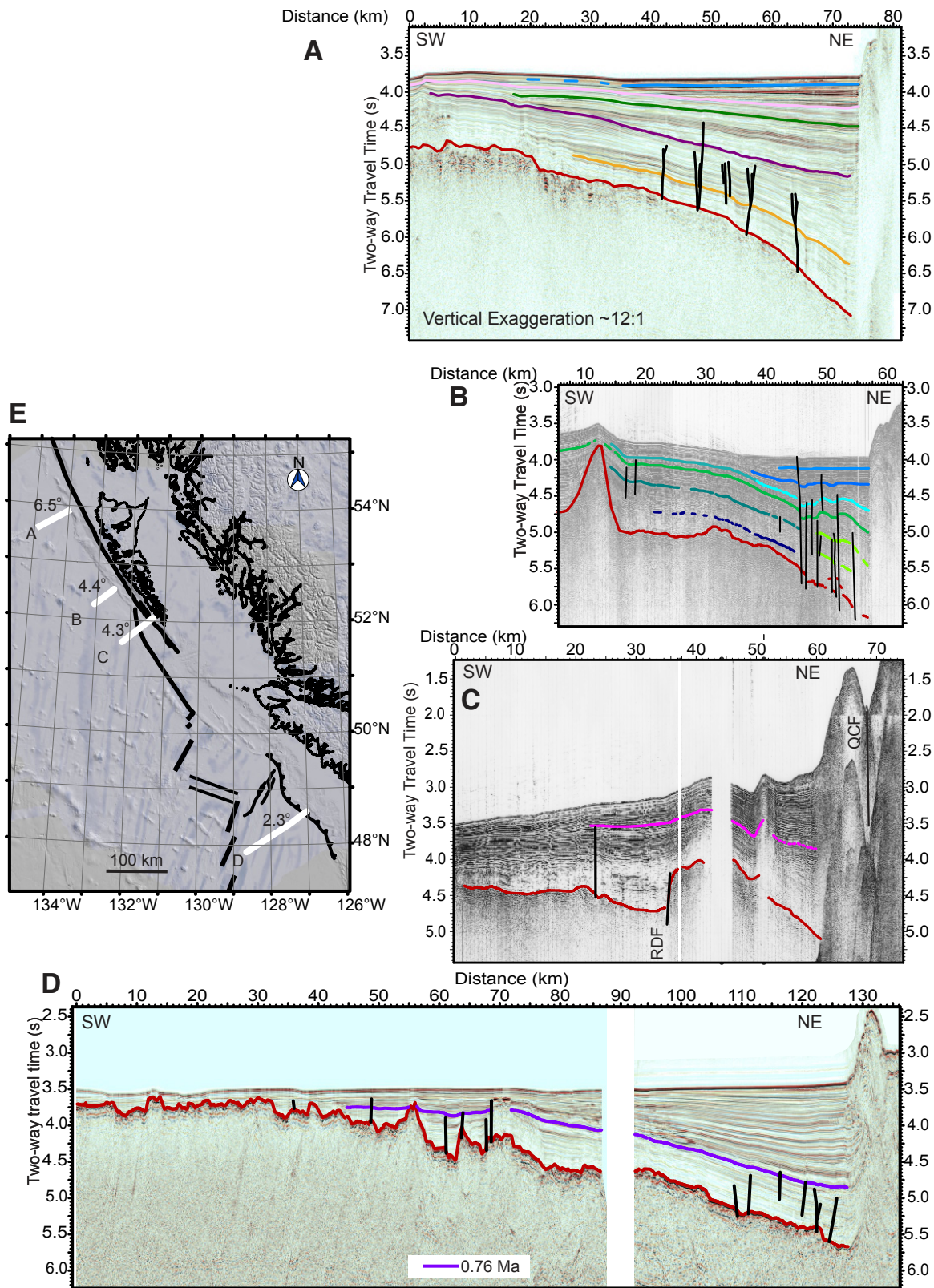
Figure 7. Seismic reflection profiles across transpressive (A–C) and subducting (D) plate boundaries drawn as in Figure 1. Locations are in panel E and Figure 1. Compression rates across Queen Charlotte fault were calculated from a geomorphic study (Brothers et al., 2019) and plate circuit poles of rotation (DeMets and Merkouriev, 2016): (A) multichannel line 77-02 (modified from Walton et al., 2015), ~14–15 Ma with compression varying from 3 to 10 mm/yr; (B) single-channel line 86-01 (Fig. 3A), ~10–11 Ma with compression of 5–15 mm/yr; (C) single-channel line 86-03 (modified from Rohr, 2015), 8–9 Ma with compression at most 5–15 mm/yr; and (D) lines 85-07 and 85-02 (modified from Rohr et al., 2019), 5–6 Ma with compression at ~35–41 mm/yr (Wilson, 2002). RDF—Revere-Dellwood fault; QCF—Queen Charlotte fault. In D, Juan de Fuca plate is subducting under North America. Dip of plate is annotated in E; in C, dip was measured between Revere-Dellwood fault and Queen Charlotte fault.

Although the 12–15 Ma Pacific plate (Fig. 7A) (Atwater and Severinghaus, 1989; Wilson, 2002) has a similar flexural wavelength to the 5–6 Ma Juan de Fuca plate (Fig. 7D), the amplitude of flexure is greater near the deformation front in part because of heavy sedimentation originating from Dixon Entrance (Walton et al., 2015). Compared to the northernmost line (Fig. 7A) the 10–11 Ma Pacific plate that is in the Queen Charlotte trough (Fig. 7B) has a shorter flexural wavelength, half the sediment thickness, and more intense faulting visible near the deformation front. Flexure imaged by line 86-3 (Fig. 7C) is strongly affected by propagation of the Revere-Dellwood fault with basement uplifted as well as being tilted down next to the Queen Charlotte fault. On the Juan de Fuca plate (Fig. 7D), much of the sediments were deposited after 0.76 Ma when the Nitinat fan began to form on the abyssal plain (Rohr et al., 2019) so the load was applied relatively recently. From north to south, respectively, dip of the oceanic plate measured on each of the lines in Figure 7 and averaged over 20 km adjacent to the deformation front is 6.5°, 4.4°, 4.3°, and 2.3°. The dip of the plate is greatest under the greatest sediment load and the least degree of compression. A compressive rate of 3–10 mm/yr (Brothers et al., 2019; DeMets and Merkouriev, 2016) was computed near 52°20′N on the Queen Charlotte fault and 35-41 mm/yr (Wilson, 2002) computed near 48°30′N on the Juan de Fuca plate. An unseen factor affecting the degree of flexure is the amount of oceanic plate underthrust or subducted beneath North America. The Juan de Fuca plate is in a well-established subduction zone whereas the Pacific plate only began underthrusting in the last 6–12 Ma (Hyndman, 2015; Schoettle-Greene et al., 2020). A quantitative analysis of flexure west of Haida Gwaii is the subject of a paper in preparation.

Trough Sedimentation

Strata below the cyan horizon (Figs. 3 and 4) thicken toward the terrace, indicating that slope fan processes, flexure, and subsidence were occurring during deposition. The single-channel seismic reflection data do not image the deepest sediments well, so angular unconformities cannot be mapped. Previous work inferred that the low-signal-to-noise section above basement consists of hemipelagic sediments (Chase and Tiffin, 1972); we note that the small amplitudes are also the result of energy attenuation from the small-volume airguns typically used.

In comparison, the shallowest horizons in the trough are variable in amplitude, are relatively flat, and onlap the landward-dipping sediments to the west. The sequence between the cyan horizon and the seafloor (Fig. 6B) has partially filled in the trough formed by the downward-flexed Pacific plate, so it thickens toward Haida Gwaii. These horizons were generally visible in all reflection data across the trough, so coverage is better than in the depth-to-basement map. The cyan horizon was taken to be the base of the sequence because it could be tracked regionally in the different data sets. The thickness between the seafloor reflector and the cyan horizon was turned into depth using the velocity function derived from an ocean-bottom seismometer located at the

base of the slope on line 13-R1 (Riedel et al., 2020). This function is somewhat slower than the function compiled from several deep global clastic sequences (Han et al., 2017), resulting in differences in computed thickness of 50 m or less.

The base of the fill sequence is deepest in the southern trough (~500 m) adjacent to the foot of the terrace and southwest of the 2012 M7.8 event. It shallows northwest along strike by ~200 m; laterally, it pinches out on the western flank of the trough. The cyan horizon could not be traced further north because the sedimentation pattern is affected by seamounts and there is a lack of tie lines. Local variations in thickness are on the order of tens of meters and are especially obvious in the south. They owe something to variations in navigation between the different surveys but are also the result of small folds and faults that deform the cyan horizon (e.g., Fig. 5).

Because sedimentary layers above the cyan horizon in the trough are relatively flat, one might infer that slope fan sedimentation has changed and/or that tectonic drivers of plate flexure have slowed or stopped altogether. However, neither relative plate motion model (DeMets and Merkouriev, 2016; Brothers et al., 2019) indicates a recent slowdown of plate motion. The presence of abundant seismicity (Earthquakes Canada, http://earthquakescanada.nrcan.gc.ca/stndon/NEDB-BNDS/bulletin-en.php) and offset gullies along the Queen Charlotte fault are also indicators of active tectonics. Therefore, we do not think that the flatness can be ascribed to a lack of tectonic activity. Given that on the Juan de Fuca plate, initiation of a slope fan has overwhelmed small tectonic signatures in the sedimentary section (Rohr et al., 2019), we explore the possibility that a local change in sedimentation regime is responsible for the trough fill sequence (Fig. 6B).

A number of canyons and gullies (Fig. 1) can transport sediment from the shelf into the trough, located (1) south of the terrace, (2) just north of the Revere-Dellwood fault, (3) west of Graham Island, and (4) on the Baranof fan. The first three sets of gullies could provide pathways, but the source in each instance is considered to be volumetrically small. Only small amounts of sediments are thought to have been input from Haida Gwaii and the terrace itself (Chase and Tiffin, 1972; Brothers et al., 2019; Barrie et al., 2013; Greene et al., 2018). The highest topography and the drainage divide are on the west coast of Haida Gwaii, so that most sediments from the islands flow eastward into Hecate Strait. From there, they flow into either the Queen Charlotte fan in the south or the Baranof fan in the north. Significant input from the Queen Charlotte fan would be captured by its deeply incised channels. However, sediment of the Baranof fan west of Dixon Entrance is several kilometers thicker than in the Queen Charlotte fan (Walton et al., 2015); glacigenic sediments from the Coast Mountains and Alaska panhandle have flowed through Dixon Entrance (Zhang and Gulick, 2019; Walton et al., 2014; Barrie et al., 2021) onto the terrace and the Pacific plate. Bathymetry of the Baranof fan shows the existence of channel-levee complexes that have deposited considerable thicknesses of sediments (Walton et al., 2015). Small channels at the very northern end of the trough can be seen in the bathymetry; they may have broken through the levees recently and fed sediments into the trough (Fig. 8C). This kind of channel avulsion is common (Pickering and Hiscott, 2016); it would focus glacial

Figure 8. Conceptual diagram of sedimentation, flexure, and deformation of Pacific plate in transpressional regime west of Haida Gwaii. (A) 10 Ma, shortly after transpression began, Pacific plate is under compression and thrust under North America, resulting in uplift of Haida Gwaii and flexure and faulting of Pacific plate. Open arrow represents approximate relative plate motion. Uplift of Haida Gwaii has blocked sediment supply coming directly from North America. Hemipelagic sediments (brown horizon) would have dominated above flexed oceanic basement (red line). (B) By 2 Ma in Quaternary, distal slope fan (green) sediments have become voluminous. At foot of slope, small landslides are indicated by irregular star shapes. Short blue arrows show landslides' direction of flow. (C) 0 Ma: Axial trough (blue) deposition has recently become significant source of sediments. Within 10–15 km of large-offset oblique thrust fault, smaller-scale normal, thrust, and strike-slip faults deform igneous oceanic crust and some of the overlying sediments. Hollow two-sided arrow in panel A represents the relative plate motion; two-sided arrows filled with light to dark grey depict sediment flow direction and one-sided black arrows depict throw on faults. Vertical exaggeration is ~6:1, or half that of seismic sections shown in Figures 3–5. At northern and southern ends of the trough, near origin points of two slope fans, trench is over-filled, whereas here, between fans, trench is underfilled. Fans provide distal deposits that blanket flexural bulge and most likely interfinger with trough deposits.
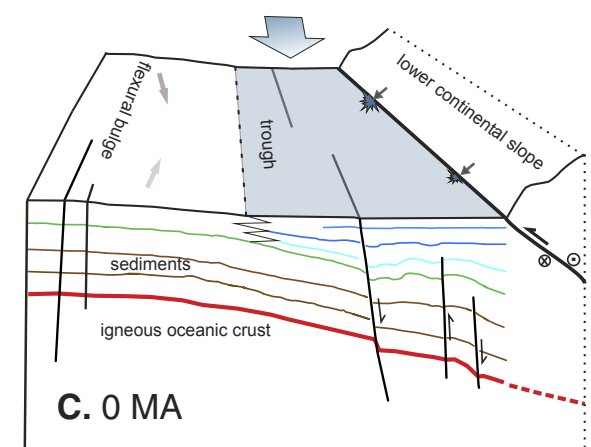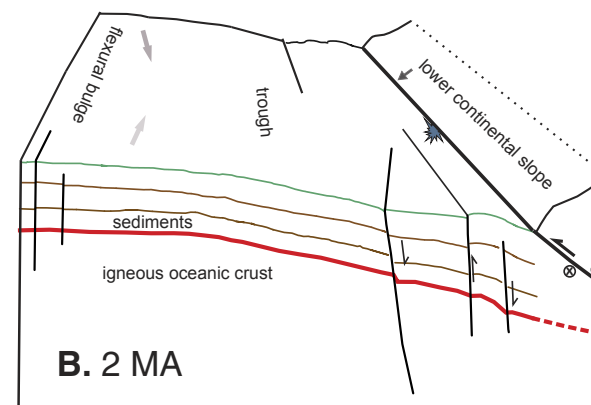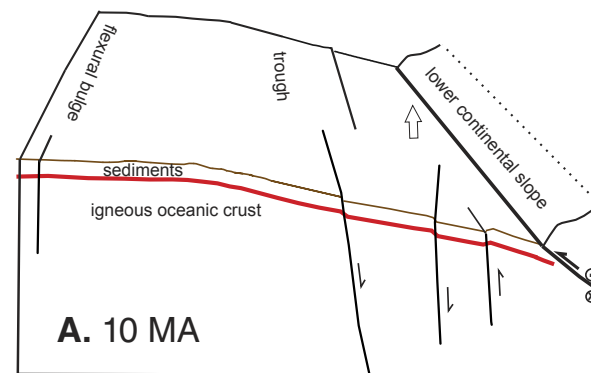
melt outflow into a trough resulting in higher depositional rates than in the wide-open geography of the abyssal plain. Higher absolute values of and greater variability in reflections' amplitudes in the fill sequence compared to amplitudes below the fill sequence (Figs. 4 and 5) imply a greater degree of contrast in physical properties of the layers, which is consistent with an origin near a source of turbidite flows. In addition, seismic velocities are lower than usual for a clastic sedimentary environment (Riedel et al., 2020); the sediments could be under-consolidated because of faster deposition. Toward the flexural bulge, trough fill deposits would be intercalated with distal deposits coming from both the Queen Charlotte and the Baranof fans such that the western edge of the trough fill is feathered and not necessarily clear cut.

Anticlines and Faults

Faults that intersect the cyan horizon are widespread, but only a few faults cut the seafloor (Fig. 6B). The latter are mainly in the southern end of the trough and coincident with vertical deflection of basement. No faults longer than the typical line spacing of 18 km can be discerned in the trough. Although it is tempting to interpret that the growth faults ~12 km from the base of the slope observed in lines 86-1 and 13-R1 (Fig. 3) are the same structure, an intervening line, 78-12170, did not image a growth fault in the projected position. Normal growth faults are likely pervasive but not necessarily long. Only two pairs of reflection lines are close enough to measure the strike of growth faults in the trough. Two faults imaged in lines 86-1 (at 45 km in Fig. 3A and line 12170 in Davis and Seemann [1981]) give an approximate north-south strike direction, which is similar to the strike of magnetic anomalies and therefore the strike of the primary extensional fault. Another fault imaged by these same lines has a strike of 285°. A fault with a strike of 325° was measured between

two lines less than 1 km apart collected during the same survey in 2013; this measurement is the most reliable. The outer edge of the terrace is aligned north-south for tens of kilometers in two places (Tréhu, et el., 2015). Extensive utilization of original oceanic faults has also been measured in the Aleutian trench (Reece et al., 2013).

Apparent dip was computed on faults observed in lines that traversed the trough using the velocity function computed from reflection and refraction data (Riedel et al., 2020). Apparent dip varied from 18° to 90° with a predominance of dip between 50° and 70°. The variety of dips observed is probably the result of the small offsets of the faults, i.e., youth of the fault system. The biggest errors in these computations are in the horizontal component, i.e., knowing exactly where each trace was located. Time is well determined.

Most of the faults observed in the reflection data have normal offsets, and many normal fault mechanisms occurred in the abundant aftershock sequence one year after the 2012 M7.8 earthquake occurred in the trough (Kao et al., 2015). In fact, most aftershocks within two months of the main shock took place in the trough in a 10–15-km-wide band at the base of the Queen Charlotte terrace (Farahbod and Kao, 2015; Riedel et al., 2020) and are coincident with faulting observed in the trough (Figs. 3–5). Only a few events occurred on the apex of the plate bend. It therefore seems logical to ascribe the origin of most of the trough events as stemming from extension of the plate as it is pulled underneath the terrace (Kao et al., 2015) rather than bending by flexure, as has been suggested (Hyndman, 2015).

A few aftershocks in the trough with strike-slip focal mechanisms (Kao et al., 2015) raise the possibility that the sediments could be deformed by strike-slip faulting. The differences in sedimentary sequences either side of the growth faults shown in Figures 3–5 could have been created by strike-slip displacement of the sediments.

Anticlines are observed in the trough and immediately adjacent to the outer faults defining the terrace. They are probably analogous to the proto-thrusts mapped in the Cascadia subduction zone (e.g., Hyndman et al., 1994), but line spacing does not allow us to measure their strike. Low signal-to-noise ratio in the deepest part of the section precludes determining if the structure continues to basement or if the décollement is shallower in the sedimentary section.

The predominance of faulting and folding in the lower sediments could imply that deformation has become less active over time or that sedimentation rate has increased. We have interpreted that the flat attitude of the shallowest horizons indicates that the fill sequence could possibly be from a sudden channel breakthrough and subsequent relatively rapid deposition of Baranof fan sediments; however, with the lack of any higher-resolution seismic data or modern bathymetric survey, this point remains somewhat speculative. A similar situation is found on the northern Juan de Fuca plate, where bending faults are not observed above the horizon that signifies initiation of the Nitinat fan (Fig. 7) (Rohr et al., 2019; Nedimović et al., 2009) and a dramatic increase in deposition rates. We infer that folding and faulting are still active in the trough, especially in the southern area offshore from the rupture plane of the 2012 M7.8 earthquake.

Fate of the Trough Sediments

Trough sediments have been incorporated into the Queen Charlotte terrace, the deformed uplifted sediments lying between the trough and Haida Gwaii (Fig. 1). It is often compared to an accretionary wedge, but we note that significant lateral transport of the sediments along the Queen Charlotte fault would have affected a number of the processes. Initially, when transpression began (6–12 Ma), mostly slowly accumulating hemipelagic sediments were present on the Pacific plate west of Haida Gwaii, so we expect that more small-offset second-order faults would have reached the seafloor in comparison to sediments deposited quickly in a fan setting (Fig. 8A). Seamounts can also act as locations of inflow and outflow of hydrothermal circulation, even over distances of 100 km or more (Davis et al., 1992). This flow could have extensively altered both the sedimentary and igneous oceanic crust that are being thrust under Haida Gwaii. Sediments on the Pacific plate approach the basal thrust obliquely; the rate perpendicular to the main fault strike is 5 km/Ma and 12 km/Ma for the geomorphic and the plate circuit models, respectively (Brothers et al., 2019; DeMets and Merkouriev, 2016). Sediments can then take 6–2.5 Ma to traverse the 30 km distance from the bulge to the base of the trough before interacting with the thrust fault underlying the terrace.

Clay minerals, which can be voluminous in the hemipelagic section, are especially important for mechanical strength in fault zones (e.g., Moore et al., 2015; Underwood et al., 2005) yet there is no information on the presence or composition of these minerals in the trough. The nearest drill site to the Queen Charlotte trough is Deep Sea Drilling Project Site 177, 200 km to the southeast; the terrigenous clastic sediments at this site contained abundant detrital and authigenic chlorite (Hayes, 1973). Recent faulting at the site likely resulted in acidic fluids circulating in the section, altering original clasts into chlorite and substantially altering the heavy mineral component as well (Scheidegger et al., 1973). This alteration could be a proxy for trench deformation that reaches the seafloor and for the more heavily faulted Queen Charlotte terrace. Additional clay minerals such as smectite and illite have been observed further afield in northeastern Pacific sediments (e.g., Blaise and Bornhold, 1987; Screaton et al., 2017).

In the Pleistocene, slope fans became very active along the shelf of British Columbia; distal flows have been deposited on the flexural bulge and in the trough (Figs. 8B and 8C). Plate motion brought Queen Charlotte slope fan sediments into the most highly transpressive region of the plate boundary. Ongoing compression folded and faulted these sediments into the terrace as seen in the proto-thrusts (Figs. 3 and 4). Whether the thrust décollement is at the top of the oceanic igneous crust or in the sedimentary stack is not clear from clear from records examined for this article. The change in sedimentary composition and depositional rate may have resulted in different mechanical properties in different layers (e.g., Han et al., 2016).

The under-consolidated trough fill sequence is most likely the unit failing at the base of slope in numerous small landslides (Fig. 8C). As the most recent deposit, they would have been involved in the most recent uplift and faulting.

The existence of these slides at this location but not in the rest of the terrace was explained (Greene et al., 2018) as resulting from a lack of hardening from earthquake shaking because they are farther from the earthquake source. With more information on the origin of these sediments, we would add the relative youth of the sediments and their uplift as reasons for these failures.

■ SUMMARY

Sediments in the Queen Charlotte trough reflect the transpressional and depositional environments (Fig. 8) as this portion of the Pacific plate interacted with North America since its formation ~450–600 km to the southeast 10–15 Ma. The cooling plate was first covered by hemipelagic sediments and later by distal flows from the Queen Charlotte and Baranof fans. The hemipelagic section in the south is less than a kilometer thick outside of the southern trough. Within ~40 km laterally of the plate boundary, the plate began to be flexed, creating a bulge and a trough (Fig. 8A). In the Quaternary, sedimentation rates increased dramatically in the fans, but ongoing uplift of Haida Gwaii and subsidence along the plate boundary fault (Queen Charlotte fault) resulted in little sedimentation flowing directly into the trough. Distal flows from the Baranof and Queen Charlotte fans were deposited on the bulge and in the trough (Fig. 8B). Recently, however, avulsion of channels in the Baranof fan possibly conducted flow into and along the trough (Fig. 8C) to nearly fill the depression with flat-lying, more variably reflective layers, as would be expected for more proximal sedimentary sequences. Seismic velocities indicate that these sediments are under-consolidated with respect to other clastic sedimentary environments (Riedel et al., 2020), which substantiates the interpretation of deposition faster than adjacent distal deposits. Such ponded flows are considered indicative of deposition rates slower than in the proximal fan but faster than in distal flows (e.g., Thornburg and Kulm, 1987). Few normal faults intersect this sequence, which is an indication of the faster sedimentation rate as well as the inability of seismic reflection data to resolve small offsets, such as at the upper tip of growth faults.

Within the trough, smaller structures have formed in response to transpression, namely small anticlines at the foot of the Queen Charlotte terrace and normal faults within the trough both from flexural bending and the slab itself being pulled underneath the terrace (Fig. 8). Landslides have been shed from the furthest outboard (and presumably youngest) faults of the terrace; they are likely from uplifted portions of this under-consolidated trough fill sequence. In the southern trough, flexure is deepest offshore and adjacent to the region of active thrusting in 2012; faults that cut the complete sedimentary column in the trough also occur in this zone of aftershocks. These observations indicate that the M7.8 2012 earthquake is representative of long-lived geologic processes.

REFERENCES CITED

Allan, J.F., Chase, R.L., Cousens, B., Michael, P.J., Gorton, M.P., and Scott, S.D., 1993, The Tuzo Wilson Volcanic Field, NE Pacific: Alkaline volcanism at a complex, diffuse, transform-trench-ridge triple junction: Journal of Geophysical Research: Solid Earth, v. 98, p. 22,367–22,387, https://doi.org/10.1029/93JB01818.

Atwater, T., and Severinghaus, J., 1989, Tectonic maps of the northeast Pacific, in Winterer, E.L., Hussong, D.M., and Decker, R.W., eds., The Eastern Pacific Ocean and Hawaii: Boulder, Colorado, Geological Society of America, Geology of North America, v. N, p. 15–20, 3 plates, https://doi.org/10.1130/DNAG-GNA-N.15.

Barrie, J.V., and Conway, K.W., 1999, Late Quaternary glaciation and postglacial stratigraphy of the northern Pacific margin of Canada: Quaternary Research, v. 51, p. 113–123, https://doi.org/10.1006/qres.1998.2021.

Barrie, J.V., Conway, K.W., and Harris, P.T., 2013, The Queen Charlotte Fault, British Columbia: Seafloor anatomy of a transform fault and its influence on sediment processes: Geo-Marine Letters, v. 33, p. 311–318, https://doi.org/10.1007/s00367-013-0333-3.

Barrie, J.V., Greene, H.G., Conway, K.W., and Brothers, D.S., 2021, Late Quaternary sea level, isostatic response, and sediment dispersal along the Queen Charlotte fault: Geosphere, v. 17, p. 375–388, https://doi.org/10.1130/GES02311.1.

Bérubé, J., Rogers, G.C., Ellis, R.M., and Hasselgren, E.O., 1989, A microseismicity study of the Queen Charlotte Islands region: Canadian Journal of Earth Sciences, v. 26, p. 2556–2566, https://doi.org/10.1139/e89-218.

Bird, A.L., 1997, Earthquakes in the Queen Charlotte Islands region: 1982–1996 [M.S. thesis]: Victoria, British Columbia, University of Victoria, 125 p.

Blaise, B., and Bornhold, B.D., 1987, Geochemistry of northern Juan de Fuca Ridge sediments, northeast Pacific: Current Research Part A: Geological Survey of Canada Paper 87-1A, p. 127–155, https://doi.org/10.4095/122477.

Brothers, D.S., Miller, N.C., Barrie, J.V., Haeussler, P.J., Greene, H.G., Andrews, B.D., Zielke, O., Watt, J., and Dartnell, P., 2019, Plate boundary localization, slip-rates and rupture segmentation of the Queen Charlotte Fault based on submarine tectonic geomorphology: Earth and Planetary Science Letters, v. 530, https://doi.org/10.1016/j.epsl.2019.115882.

Bruns, T.R., Stevenson, A.J., and Dobson, M.R., 1992, GLORIA investigation of the Exclusive Economic Zone in the Gulf of Alaska and off southeast Alaska; M/V Farnella Cruise F7-89-GA, June 14–July 13, 1989: U.S. Geological Survey Open-File Report 92-317, 16 p., https://doi.org/10.3133/ofr92317.

Carbotte, S.M., Dixon, J.M., Farrar, E., Davis, E.E., and Riddihough, R.P., 1989, Geological and geophysical characteristics of the Tuzo Wilson Seamounts: Implications for plate geometry in the vicinity of the Pacific–North America–Explorer triple junction: Canadian Journal of Earth Sciences, v. 26, p. 2365–2384, https://doi.org/10.1139/e89-202.

Cassidy, J.F., Rogers, G.C., and Hyndman, R.D., 2014, An overview of the 28 October 2012 M_w 7.7 earthquake in Haida Gwaii, Canada: A tsunamigenic thrust event along a predominantly strike-slip margin: Pure and Applied Geophysics, v. 171, p. 3457–3465, https://doi.org/10.1007/s00024-014-0775-1.

Chase, R.L., and Tiffin, D.L., 1972, Queen Charlotte fault zone, British Columbia, in Gill, J.E., Béland, J., and Mountjoy, E.W., eds., International Geological Congress, Twenty-Fourth Session: Montréal, International Geological Congress, v. 8, p. 17–27.

Chaytor, J.D., Keller, R.A., Duncan, R.A., and Dziak, R.P., 2007, Seamount morphology in the Bowie and Cobb hot spot trails, Gulf of Alaska: Geochemistry, Geophysics, Geosystems, v. 8, Q09016, https://doi.org/10.1029/2007GC001712.

Davis, E.E., and Seemann, D.A., 1981, A compilation of seismic reflection profiles across the continental margin of western Canada: Geological Survey of Canada Open File 751, 9 plates, https://doi.org/10.4095/129686.

Davis, E.E., et al., 1992, FlankFlux: An experiment to study the nature of hydrothermal circulation in young oceanic crust: Canadian Journal of Earth Sciences, v. 29, p. 925–952, https://doi.org/10.1139/e92-078.

DeMets, C., and Merkouriev, S., 2016, High-resolution reconstructions of Pacific–North America plate motion: 20 Ma to present: Geophysical Journal International, v. 207, p. 741–773, https://doi.org/10.1093/gji/ggw305.

Farahbod, A.M., and Kao, H., 2015, Spatiotemporal distribution of events during the first week of the 2012 Haida Gwaii aftershock sequence: Bulletin of the Seismological Society of America, v. 105, p. 1231–1240, https://doi.org/10.1785/0120140173.

Ferguson, R., King, H.M., Kublik, K., Rohr, K.M.M., Kung, L., Lister, C.J., Fustic, M., Hayward, N., Brent, T.A., and Jassim, Y., 2018, Petroleum, mineral, and other resource potential in the offshore Pacific, British Columbia, Canada: Geological Survey of Canada Open File 8390, 82 p., https://doi.org/10.4095/308395.

Greene, H.G., et al., 2018, Slope failure and mass transport processes along the Queen Charlotte Fault Zone, western British Columbia, in Lintern, D.G., et al., eds., Subaqueous Mass Movements and their Consequences: Assessing Geohazards, Environmental Implications and Economic Significance of Subaqueous Landslides: Geological Society of London Special Publication 477, p. 85–106, https://doi.org/10.1144/SP477.31.

Han, S., Carbotte, S.M., Canales, J.P., Nedimović, M.R., Carton, H., Gibson, J.C., and Horning, G.W., 2016, Seismic reflection imaging of the Juan de Fuca plate from ridge to trench: New constraints on the distribution of faulting and evolution of the crust prior to subduction: Journal of Geophysical Research: Solid Earth, v. 121, p. 1849–1872, https://doi.org/10.1002/2015JB012416.

Han, S., Bangs, N.L., Carbotte, S.M., Saffer, D.M., and Gibson, J.C., 2017, Links between sediment consolidation and Cascadia megathrust slip behaviour: Nature Geoscience, v. 10, p. 954–959, https://doi.org/10.1038/s41561-017-0007-2.

Harris, P.T., Barrie, J.V., Conway, K.W., and Greene, H.G., 2014, Hanging canyons of Haida Gwaii, British Columbia, Canada: Fault-control on submarine canyon geomorphology along active continental margins: Deep-Sea Research II, v. 104, p. 83–92, http://doi.org/10.1016/j.dsr2.2013.06.017.

Harris, R.N., and Chapman, D.S., 1994, A comparison of mechanical thickness estimates from trough and seamount loading in the southeastern Gulf of Alaska: Journal of Geophysical Research: Solid Earth, v. 99, p. 9297–9317, https://doi.org/10.1029/93JB03285.

Hayes, J.B., 1973, Petrology of indurated sandstones, Leg 18, Deep Sea Drilling Project, in Kulm, L.D., von Hume, R., et al., Initial Reports of the Deep Sea Drilling Project, Volume 18: Washington, D.C., U.S. Government Printing Office, p. 915–924, https://doi.org/10.2973/dsdp.proc.18.129.1973.

Hyndman, R.D., 2015, Tectonics and structure of the Queen Charlotte fault zone, Haida Gwaii, and large thrust earthquakes: Bulletin of the Seismological Society of America, v. 105, p. 1058–1075, https://doi.org/10.1785/0120140181.

Hyndman, R.D., and Ellis, R.M., 1981, Queen Charlotte fault zone: Microearthquakes from a temporary array of land stations and ocean bottom seismographs: Canadian Journal of Earth Sciences, v. 18, p. 776–788, https://doi.org/10.1139/e81-071.

Hyndman, R.D., Spence, G.D., Yuan, T., and Davis, E.E., 1994, Regional geophysics and structural framework of the Vancouver Island margin accretionary prism, in Westbrook, G.K., Carson, B., Musgrave, R.J., et al., Proceedings of the Ocean Drilling Program, Initial Reports, Volume 146 (Part 1): College Station, Texas, Ocean Drilling Program, p. 399–419, https://doi.org/10.2973/odp.proc.ir.146-1.002.1994.

Kao, H., Shan, S.-J., and Farahbod, A.M., 2015, Source characteristics of the 2012 Haida Gwaii earthquake sequence: Bulletin of the Seismological Society of America, v. 105, p. 1206–1218, https://doi.org/10.1785/0120140165.

Moore, J.C., Plank, T.A., Chester, F.M., Polissar, P.J., and Savage, H.M., 2015, Sediment provenance and controls on slip propagation: Lessons learned from the 2011 Tohoku and other great earthquakes of the subducting northwest Pacific plate: Geosphere, v. 11, p. 533–541, https://doi.org/10.1130/GES01099.1.

Nedimović, M.R., Bohnenstiehl, D.R., Carbotte, S.M., Canales, J.P., and Dziak, R.P., 2009, Faulting and hydration of the Juan de Fuca plate system: Earth and Planetary Science Letters, v. 284, p. 94–102, https://doi.org/10.1016/j.epsl.2009.04.013.

Nilsen, T.H., and McLaughlin, R.J., 1985, Comparison of tectonic framework and depositional patterns of the Hornelen strike-slip basin of Norway and the Ridge and Little Sulphur Creek strike-slip basins of California, in Biddle, K.T., and Christie-Blick, N., eds., Strike-Slip Deformation, Basin Formation, and Sedimentation, Society of Economic Paleontologists and Mineralogists Special Publication 37, p. 79–103, https://doi.org/10.2110/pec.85.37.0079.

Norgard, T., et al., 2019, Northeast Pacific Seamount Expedition: Exploring Canada's seamounts, in Raineault, N.A., and Flanders, J., eds., New Frontiers in Ocean Exploration: Oceanography, v. 32, Suppl., p. 42–43, https://doi.org/10.5670/oceanog.2019.supplement.01.

Normark, W.R., Piper, D.J.W., Posamentier, H., Pirmez, C., and Migeon, S., 2002, Variability in form and growth of sediment waves on turbidite channel levees: Marine Geology, v. 192, p. 23–58, https://doi.org/10.1016/S0025-3227(02)00548-0.

Nykolaishen, L., Dragert, H., Wang, K., James, T.S., and Schmidt, M., 2015, GPS observations of crustal deformation associated with the Mw 7.8 Haida Gwaii Earthquake: Bulletin of the Seismological Society of America, v. 105, p. 1241–1252, https://doi.org/10.1785/0120140177.

Pickering, K.T., and Hiscott, R.N., 2016, Deep Marine Systems: Processes, Deposits, Environments, Tectonics and Sedimentation: Chichester, UK, American Geophysical Union and John Wiley & Sons, 688 p.

Prims, J., Furlong, K.P., Rohr, K.M.M., and Govers, R., 1997, Lithospheric structure along the Queen Charlotte margin in western Canada: Constraints from flexural modeling: Geo-Marine Letters, v. 17, p. 94–99, https://doi.org/10.1007/s003670050013.

Reece, R.S., Gulick, S.P.S., Christeson, G.L., Horton, B.K., van Avendonk, H., and Barth, G., 2013, The role of far field tectonic stress in oceanic intraplate deformation, Gulf of Alaska: Journal of Geophysical Research: Solid Earth, v. 118, p. 1862–1872, https://doi.org/10.1002/jgrb.50177.

Riedel, M., Côté, M.M., and Neelands, P.J., 2014, Cruise report PGC2013001PGC—The Mw 7.7 Haida Gwaii Earthquake ocean bottom seismometer experiment: Instrument recovery and active-source seismic refraction experiment, CCG Vessel John P. Tully, 7–14 January, 2013: Geological Survey of Canada Open File 7556, 41 p., https://doi.org/10.4095/293917.

Riedel, M., Rohr, K.M.M., Côté, M.M., Schmidt, U., and Richardson, T., 2019, Gas hydrate occurrences along the Haida Gwaii margin—Constraints on the geothermal regime and implications for fluid flow: Geosphere, v. 16, p. 1–12, https://doi.org/10.1130/GES02103.1.

Riedel, M., Yelisetti, S., Papenberg, C., Rohr, K.M.M., Côté, M.M., Spence, G.D., Hyndman, R.D., and James, T., 2020, Seismic velocity structure of the Queen Charlotte terrace off western Canada in the region of the 2012 Haida Gwaii Mw 7.8 thrust earthquake: Geosphere, v. 17, p. 23–38, https://doi.org/10.1130/GES02258.1.

Ristau, J.R., Rogers, G.C., and Cassidy, J.F., 2007, Stress in western Canada from regional moment tensor analysis: Canadian Journal of Earth Sciences, v. 44, p. 127–148, https://doi.org/10.1139/e06-057.

Rohr, K.M.M., 2015, Plate boundary adjustments of the southernmost Queen Charlotte fault: Bulletin of the Seismological Society of America, v. 105, p. 1076–1089, https://doi.org/10.1785/0120140162.

Rohr, K.M.M., and Dietrich, J.R., 1992, Strike slip tectonics and development of the Tertiary Queen Charlotte basin, offshore western Canada: Evidence from seismic reflection data: Basin Research, v. 4, p. 1–20, https://doi.org/10.1111/j.1365-2117.1992.tb00039.x.

Rohr, K.M.M., and Furlong, K.P., 1995, Ephemeral plate tectonics at the Queen Charlotte triple junction: Geology, v. 23, p. 1035–1038, https://doi.org/10.1130/0091-7613(1995)023<1035:EPTATQ>2.3.CO;2.

Rohr, K.M.M., King, H., Riedel, M., and Schmidt, U., 2019, From mid-plate to subduction zone: Stratigraphy of the northeast Juan de Fuca Plate, offshore British Columbia: Geological Survey of Canada Current Research Paper 2019-4, 17 p., https://doi.org/10.4095/314906

Ryan, W.B.F., et al., 2009, Global Multi-Resolution Topography (GMRT) synthesis: Geochemistry, Geophysics, Geosystems, v. 10, Q03014, https://doi.org/10.1029/2008GC002332.

Scheidegger, K.F., Kulm, L.D., and Piper, D.J.W., 1973, Heavy mineralogy of unconsolidated sands in northeastern Pacific sediments: Leg 18, Deep Sea Drilling Project, in Kulm, L.D., von Huene, R., et al., Initial Reports of the Deep Sea Drilling Project, Volume 18: Washington, D.C., U.S. Government Printing Office, p. 877–887, https://doi.org/10.2973/dsdp.proc.18.125.1973.

Schoettle-Greene, P., Duval, A.R., Blythe, A., Morley, E., Matthews, W., and LaHusen, S.R., 2020, Uplift and exhumation in Haida Gwaii driven by terrane translation and transpression along the southern Queen Charlotte fault, Canada: Geology, v. 48, p. 908–912, https://doi.org/10.1130/G47364.1.

Screaton, E.J., Villaseñor, T., James, S.R., Meridth, L.N., Jaeger, J.M., and Kenney, W.F., 2017, Data report: Permeability, grain size, biogenic silica, and clay minerals of Expedition 341

sediments from Sites U1417 and U1418, *in* Jaeger, J.M., Gulick, S.P.S., LeVay, L.J., and the Expedition 341 Scientists, Proceedings of the Integrated Ocean Drilling Program, Volume 341: College Station, Texas, Integrated Ocean Drilling Program, https://doi.org/10.2204/iodp.proc.341.202.2017.

Srivastava, S.P., Chase, D.L., Keen, C.E., Manchester, K.S., Shaw, K.G., Tiffin, D.L., Chase, R.L., Thomlinson, A.G., Davis, E.E., and Lister, C.R.B., 1971, Preliminary analysis of geophysical measurements north of Juan de Fuca Ridge: Canadian Journal of Earth Sciences, v. 8, p. 1265–1281, https://doi.org/10.1139/e71-115.

Thornburg, T.M., and Kulm, L.D., 1987, Sedimentation in the Chile Trench: Depositional morphologies, lithofacies, and stratigraphy: Geological Society of America Bulletin, v. 98, p. 33–52, https://doi.org/10.1130/0016-7606(1987)98<33:SITCTD>2.0.CO;2.

Tréhu, A.M., Scheidhauer, M., Rohr, K.M.M., Tikoff, B., Walton, M.A.L., Gulick, S.P.S., and Roland, E.C., 2015, An abrupt transition in the mechanical response of the upper crust to transpression along the Queen Charlotte fault: Bulletin of the Seismological Society of America, v. 105, p. 1114–1128, https://doi.org/10.1785/0120140159.

Underwood, M.B., Hoke, K.D., Fisher, A.T., Davis, E.E., Giambalvo, E., Zühlsdorff, L., and Spinelli, G.A., 2005, Provenance, stratigraphic architecture, and hydrogeologic influence of turbidites on the mid-ocean ridge flank of northwestern Cascadia Basin, Pacific Ocean: Journal of Sedimentary Research, v. 75, p. 149–164, https://doi.org/10.2110/jsr.2005.012.

Walton, M.A.L., Gulick, S.P.S., Reece, R.S., Barth, G.A., Christeson, G.L., and van Avendonk, H.J.A., 2014, Dynamic response to strike-slip tectonic control on the deposition and evolution of the Baranof Fan, Gulf of Alaska: Geosphere, v. 10, p. 680–691, https://doi.org/10.1130/GES01034.1.

Walton, M.A.L., Gulick, S.P.S., Haeussler, P.J., Roland, E.C., and Tréhu, A.M., 2015, Basement and regional structure along-strike of the Queen Charlotte fault in the context of modern and historical earthquake ruptures: Bulletin of the Seismological Society of America, v. 105, p. 1090–1105, https://doi.org/10.1785/0120140174.

Wilson, D.S., 2002, The Juan de Fuca plate and slab: Isochron structure and Cenozoic plate motions, *in* Kirby, S., Wang, K., and Dunlop, S., eds., The Cascadia Subduction Zone and Related Subduction Systems: Geological Survey of Canada Open File 4350, p. 19–22, https://doi.org/10.4095/222387.

Wilson, J.T., 1965, A new class of faults and their bearing on continental drift: Nature, v. 207, p. 343–347, https://doi.org/10.1038/207343a0.

Woodsworth, G.J., ed., 1991, Evolution and hydrocarbon potential of the Queen Charlotte Basin, British Columbia: Geological Survey of Canada Paper 90-10, 569 p., https://doi.org/10.4095/131959.

Wynn, R.B., and Stow, D.A.V., 2002, Classification and characterisation of deep-water sediment waves: Marine Geology, v. 192, p. 7–22, https://doi.org/10.1016/S0025-3227(02)00547-9.

Zhang, J., and Gulick, S.P.S., 2019, Sequence stratigraphy and depositional history of the Baranof Fan: Insights for Cordilleran Ice Sheet outflow to the Gulf of Alaska: Geological Society of America Bulletin, v. 132, p. 353–372, https://doi.org/10.1130/B35164.1.